High optical polarization ratio from semipolar $(20\bar{2}\bar{1})$ blue-green InGaN/GaN light-emitting diodes

Yuji Zhao,[1,a)] Shinichi Tanaka,[2] Qimin Yan,[2] Chia-Yen Huang,[2] Roy B. Chung,[2] Chih-Chien Pan,[2] Kenji Fujito,[3] Daniel Feezell,[2] Chris G. Van de Walle,[2] James S. Speck,[2] Steven P. DenBaars,[1,2] and Shuji Nakamura[1,2]
[1]*Electrical and Computer Engineering Department, University of California, Santa Barbara, California 93106, USA*
[2]*Materials Department, University of California, Santa Barbara, California 93106, USA*
[3]*Optoelectronic Laboratory, Mitsubishi Chemical Corporation, 1000 Higashi-Mamiana, Ushiku, Ibaraki 300-1295, Japan*

(Received 19 June 2011; accepted 11 July 2011; published online 3 August 2011; publisher error corrected 8 August 2011)

The optical polarization ratio of spontaneous emission was investigated by electroluminescence measurements for semipolar $(20\bar{2}\bar{1})$ InGaN/GaN light-emitting diodes, covering the blue to green spectral range. Devices fabricated on semipolar $(20\bar{2}\bar{1})$ substrates exhibit polarization ratios ranging from 0.46 at 418 nm to 0.67 at 519 nm. These polarization ratios are significantly higher than those reported on semipolar $(20\bar{2}1)$ devices. The valence band energy separation is extracted from spectral measurements and is consistent with the increased polarization ratio and theoretical predictions. Quantum well interdiffusion induced valence band mixing is suggested as a possible explanation for the low experimental value of polarization ratio observed for the $(20\bar{2}1)$ devices. © *2011 American Institute of Physics*. [doi:10.1063/1.3619826]

Semipolar and nonpolar orientations of group III-Nitrides have attracted considerable attention for realizing high-efficiency light-emitting diodes (LEDs) (Ref. 1) and laser diodes (LDs).[2] Several advantages over commercially available *c*-plane structures have been highlighted, including reduced polarization-induced electric fields in the quantum wells (QWs),[3–5] increased indium uptake,[6–8] and polarized light emission.[9–11] The former characteristics are promising for achieving high-performance green emitters, while the latter characteristic contributes to anisotropic optical gain in LDs fabricated on these planes.[12] For example, on nonpolar (*m*-plane), the emission components polarized along the *a*- and *c*-axes involve the highest and second highest valence bands, respectively. Due to the higher emission intensity along the *a*-axis,[13] LD stripes oriented along the *c*-axis exhibit a lower threshold current, and they are thus preferred on *m*-plane GaN.[14] The relative magnitude of the intensity parallel to and perpendicular to the *c*-axis is described by the polarization ratio, and high values are desired for improved LD performance. Similar optical gain anisotropy and threshold behavior have also been observed for devices on semipolar $(11\bar{2}2)$[15,16] and $(20\bar{2}1)$.[17]

While high polarization ratios have been reported for *m*-plane devices,[18,19] long wavelength emission is difficult to achieve on this plane due to the generation of defects inside the QWs at high indium compositions.[20] The semipolar $(20\bar{2}1)$ orientation has recently shown promising performance at long wavelengths, but the reported polarization ratios are relatively low.[17] In this work, we report increased polarization ratios of LED devices on the $(20\bar{2}\bar{1})$ semipolar plane, which is inclined at 15° and 30° toward the $[000\bar{1}]$ direction from the *m*-plane and the$(20\bar{2}1)$plane, respectively. Using integrated electroluminescence (EL) measurements, the polarization ratio was 0.67 at 519 nm for $490 \times 292\ \mu m^2$ $(20\bar{2}\bar{1})$ devices at 20 mA. Comparable devices of a similar wavelength on the $(20\bar{2}1)$ plane showed a polarization ratio of 0.34.

LEDs were homoepitaxially grown by conventional metal organic chemical vapor deposition (MOCVD) on free-standing $(20\bar{2}\bar{1})$ GaN substrates supplied by Mitsubishi Chemical Corporation. The device structure consists of a 1 μm Si-doped *n*-type GaN layer, a multiple quantum well (MQW) active region consisting of three periods of InGaN (3 nm)/GaN (16 nm), a 16 nm Mg-doped $Al_{0.15}Ga_{0.85}N$ electron blocking layer (EBL), and a 60 nm *p*-type GaN layer. For the LED fabrication, a rectangular mesa pattern ($490 \times 292\ \mu m^2$) was formed by conventional lithography and chlorine-based inductively coupled plasma (ICP) etching after an indium tin oxide (ITO) current spreading layer was deposited by electron beam evaporation. Ti/Al/Ni/Au *n*-type contacts and Ti/Au pads were deposited by electron beam evaporation and a conventional lift-off process. Next, black ink was applied to the bottom and side surfaces of the devices as a photon absorbing element to prevent multiple reflections. A group of semipolar $(20\bar{2}1)$ LEDs with the same device structure were also fabricated and characterized as reference samples. The schematic views for the$(20\bar{2}1)$, $(20\bar{2}\bar{1})$, and *m*-plane orientations in the wurtzite crystal structure are presented in Fig. 1.

EL measurements were carried out under direct current (DC) operation at room temperature using a 0.45 numerical aperture 20× microscope objective designed for collection of polarized light. The details of the experimental setup can be found in Ref. 21. The optical polarization ratio (ρ), given by $\rho = (I_{[\bar{1}2\bar{1}0]} - I_{[\bar{1}01\bar{4}]})/(I_{[\bar{1}2\bar{1}0]} + I_{[\bar{1}01\bar{4}]})$, where $I_{[\bar{1}2\bar{1}0]}$ and $I_{[\bar{1}01\bar{4}]}$ are the integrated EL intensities with the polarizer aligned along the $[\bar{1}2\bar{1}0]$ and $[\bar{1}01\bar{4}]$ directions of the sample, respectively, is plotted in Fig. 2(a). For highly inclined semipolar planes such as $(20\bar{2}1)$ and $(20\bar{2}\bar{1})$, the energy

a)Electronic mail: yujizhao@engineering.ucsb.edu.

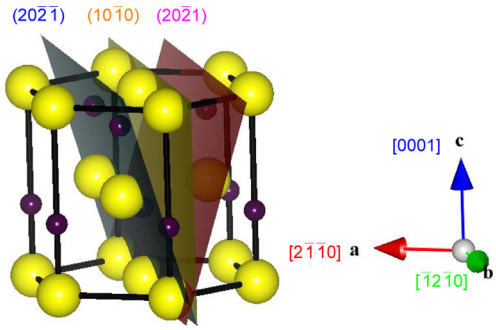

FIG. 1. (Color online) The schematic views for different crystal planes of (20$\bar{2}\bar{1}$), (20$\bar{2}$1), and *m*-plane in wurtzite crystal structure.

separation between the top two valence bands (ΔE) is approximately given by the energy difference between emission peak wavelengths for the two polarizations.[22] This energy separation is plotted in Fig. 3(c) and is discussed below.

Fig. 2(a) shows the polarization ratio of LEDs fabricated on (20$\bar{2}\bar{1}$) free-standing GaN substrates as a function of the peak wavelength of the dominant emission component, while Fig. 2(b) illustrates the polarization ratio as a function of current density (from 10.5 A/cm^2 to 55.9 A/cm^2). Polarization ratios beyond 60 A/cm^2 were not extracted in order to avoid excessive device heating. The polarization ratio was found to be nearly independent of electrical bias, possibly indicating high compositional uniformity for (20$\bar{2}\bar{1}$) InGaN QWs. Previously reported polarization ratio data for MQWs with 3–4 nm QWs on *m*-plane[11,18] (obtained by photoluminescence (PL)) and for MQWs with 3–4 nm QWs on the (20$\bar{2}$1) plane[17] (measured under a current density of 7.4 A/cm^2) are also plotted in Fig. 2(a). Additionally, reference (20$\bar{2}$1) samples were grown, fabricated, and measured under the same conditions as the (20$\bar{2}\bar{1}$) samples reported here, and the data

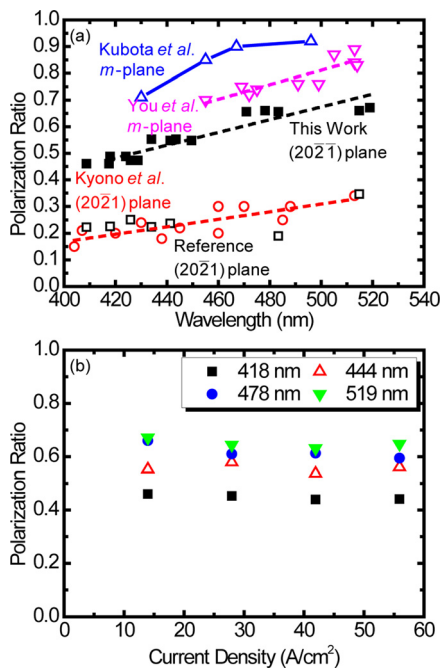

FIG. 2. (Color online) (a) Polarization ratio of the LEDs on (20$\bar{2}\bar{1}$) plane GaN substrates as a function of the peak wavelength of the dominant emission component. (b) Polarization ratio of the LEDs on (20$\bar{2}\bar{1}$) plane GaN substrates as a function of different current densities.

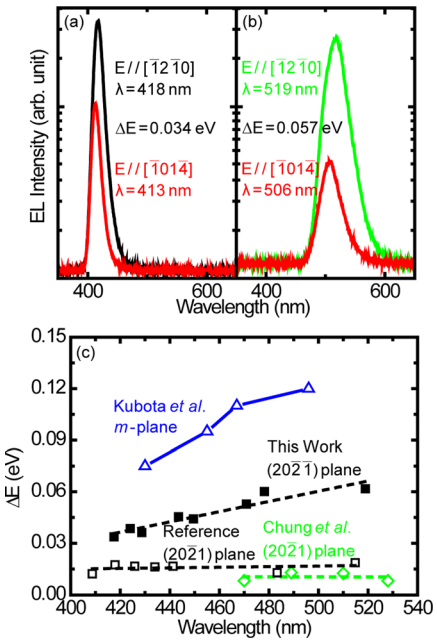

FIG. 3. (Color online) EL spectra of (20$\bar{2}\bar{1}$) LEDs at a wavelength of (a) 418 nm, (b) 519 nm, and (c) energy separation (ΔE) with increasing wavelength on (20$\bar{2}\bar{1}$) plane devices.

is included in Fig. 2(a). The results obtained for the (20$\bar{2}$1) reference samples are in good agreement with previously reported data, indicating that variations due to experimental configurations are insignificant. The polarization ratio on the (20$\bar{2}\bar{1}$) plane shows a monotonic increase with wavelength, which is in agreement with experimental results.[11] While the peak wavelength dependence for the (20$\bar{2}\bar{1}$) plane is similar to that of *m*-plane and (20$\bar{2}$1), the devices on (20$\bar{2}\bar{1}$) show a much larger polarization ratio than those on the (20$\bar{2}$1) plane. It has been theoretically predicted and experimentally verified that a high polarization ratio is preferable for achieving increased optical gain in laser diodes.[12] Devices grown on semipolar (20$\bar{2}\bar{1}$) exhibit high polarization ratios compared to those on (20$\bar{2}$1) and, therefore, may facilitate improved LD performance in the green spectral region.[14–17]

Figs. 3(a) and 3(b) show the EL spectra of (20$\bar{2}\bar{1}$) LEDs at wavelengths of 418 nm and 519 nm, respectively. The emission component polarized along the [$\bar{1}$2$\bar{1}$0] plane is dominant, as indicated by the higher intensity compared to that of the component polarized along the [$\bar{1}$01$\bar{4}$] plane. The intensity difference between the two components becomes larger as the wavelength increases, which is in good agreement with theory.[23] It is also noteworthy that the switching phenomenon that was reported for (11$\bar{2}\bar{2}$) InGaN QWs (Refs. 24 and 25) was not observed for (20$\bar{2}\bar{1}$) nor (20$\bar{2}$1) devices. Fig. 3(c) shows the energy separation (ΔE) versus wavelength for devices on semipolar (20$\bar{2}\bar{1}$). Previously reported values on *m*-plane[11] and the (20$\bar{2}$1) plane,[26] as well as data from reference (20$\bar{2}$1) devices, are also plotted. All the data show an increasing ΔE with increasing wavelength, which is again in good agreement with theoretical predictions.[13] It is anticipated that by incorporating more indium in the QWs, the in-plane anisotropic strain increases and thus it further splits the valence bands. The (20$\bar{2}\bar{1}$) devices show a higher degree of band splitting compared to (20$\bar{2}$1) devices, which is consistent with the results obtained for polarization ratio.

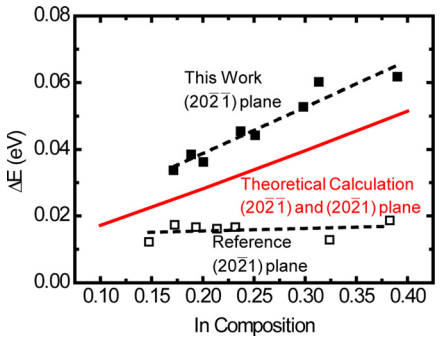

FIG. 4. (Color online) The energy separation (ΔE) between the top two valence bands at the Γ point for 3 nm (20$\bar{2}$1) semipolar InGaN QW strained on GaN with different In compositions obtained by the k·p method using NEXTNANO3 software. The experimental data on (20$\bar{2}$1) and (20$\bar{2}$1) are also plotted for comparison, where the In composition is determined by assuming Vegard's law.

To examine the experimentally obtained energy differences, the energy separation between the top two valence bands at the Γ point for 3 nm (20$\bar{2}$1) semipolar InGaN QW strained on GaN with different In compositions was obtained by the k·p method using the NEXTNANO3 software,[27] and is shown in Fig. 4. The experimental data on (20$\bar{2}$1) and (20$\bar{2}$1) are also plotted for comparison, where the In composition was determined by using Vegard's law. Note that the simulation predicts identical separations between the top two valence bands for (20$\bar{2}$1) and (20$\bar{2}$1), and that the values obtained for (20$\bar{2}$1) are close to a previous report.[23] Due to the quantum confinement effect, the band separation between the top two valence subbands in (20$\bar{2}$1) and (20$\bar{2}$1) QWs is slightly larger than that of the bulk InGaN case. The experimental data obtained for the (20$\bar{2}$1) plane is in reasonable agreement with the simulation, while that of the (20$\bar{2}$1) plane is significantly smaller. Since the strain profiles for QWs on (20$\bar{2}$1) and (20$\bar{2}$1) are identical, such a discrepancy is attributed to a difference in the microscopic structure of the InGaN QWs. As suggested theoretically for InGaAs/InP quantum wells,[28–31] the interdiffusion of In and Ga atoms may play a critical role by changing the indium compositional profile in the QWs, leading to a modification of the valence subband structures. The difference in compositional profile will modify the valence subband structures by changing the subband separation and the effective mass of each band. We propose that the QWs structure grown on the (20$\bar{2}$1) plane may be degraded by such interdiffusion. A decrease of the subband separation in the QWs would induce a decrease in the polarization ratio for the (20$\bar{2}$1) plane. Such a difference is likely due to the different growth mechanisms on these two planes, which has been observed and will be reported elsewhere.[32] A more systematic study, including transmission electron microscopy (TEM) and atom probe analysis, of structural properties and chemical composition profiles for QWs on these planes is a topic of ongoing investigation.

In summary, we have grown and fabricated LEDs on the semipolar (20$\bar{2}$1) plane with emission wavelengths ranging from blue to green. These devices have shown high optical polarization ratios and large valence band separations compared to reference devices grown on semipolar (20$\bar{2}$1). The results obtained for LEDs on the (20$\bar{2}$1) plane are in reasonable agreement with simulated values obtained by the k·p method. The low experimental values observed on the (20$\bar{2}$1) plane may be due to valence band mixing caused by QW interdiffusion due to the different growth mechanisms on the two planes. This is a topic of ongoing investigation.

Y. Zhao would like to thank Stuart Brinkley, Nathan Pfaff, and Christopher Keraly for the helpful discussion. The authors acknowledge the support of Solid State Lighting and Energy Center at UCSB. A portion of this work was done in the UCSB nanofabrication facility, part of the National Science Foundation (NSF) funded National Nanotechnology Infrastructure Network (NNIN).

[1]Y. Zhao, J. Sonoda, C. C. Pan, S. Brinkley, I. Koslow, K. Fujito, H. Ohta, S. P. DenBaars, and S. Nakamura, Appl. Phys. Express **3**, 102101 (2010).
[2]J. W. Raring, M. C. Schmidt, C. Poblenz, Y. C. Chang, M. J. Mondry, B. Li, J. Iveland, B. Walters, M. R. Krames, R. Craig, P. Rudy, J. S. Speck, S. P. DenBaars, and S. Nakamura, Appl. Phys. Express **3**, 112101 (2010).
[3]P. Waltereit, O. Brandt, A. Trampert, H. T. Grahn, J. Menniger, M. Ramsteiner, M. Reiche, and K. H. Ploog, Nature (London) **406**, 865 (2000).
[4]M. C. Schmidt, K. C. Kim, H. Sato, N. Fellows, H. Masui, S. Nakamura, S. P. DenBaars, and J. S. Speck, Jpn. J. Appl. Phys. **46**, L126 (2007).
[5]Y. Zhao, J. Sonoda, I. Koslow, C. C. Pan, H. Ohta, J. S. Ha, S. P. Denbaars, and S. Nakamura, Jpn. J. Appl. Phys. **49**, 070206 (2010).
[6]Y. Enya, Y. Yoshizumi, T. Kyono, K. Akita, M. Ueno, M. Adachi, T. Sumitomo, S. Tokuyama, T. Ikegami, K. Katayama, and T. Nakamura, Appl. Phys. Express **2**, 082101 (2009).
[7]Y. D. Lin, S. Yamamoto, C. Y. Huang, C. L. Hsiung, F. Wu, K. Fujito, H. Ohta, J. S. Speck, S. P. Denbaars, and S. Nakamura, Appl. Phys. Express **3**, 082001 (2010).
[8]S. Yamamoto, Y. Zhao, C. C. Pan, R. B. Chung, K. Fujito, J. Sonoda, S. P. Denbaars, and S. Nakamura, Appl. Phys. Express **3**, 122102 (2010).
[9]N. F. Gardner, J. C. Kim, J. J. Wierer, Y. C. Shen, and M. R. Krames, Appl. Phys. Lett. **86**, 111101 (2005).
[10]H. Masui, H. Yamada, K. Iso, S. Nakamura, and S. P. Denbaars, Appl. Phys. Lett. **92**, 091105 (2008).
[11]M. Kubota, K. Okamoto, T. Tanaka, and H. Ohta, Appl. Phys. Lett. **92**, 011920 (2008).
[12]S. H. Park and D. Ahn, Appl. Phys. Lett. **90**, 013505 (2007).
[13]T. Ohtoshi, A. Niwa, and T. Kuroda, J. Appl. Phys. **82**, 1518 (1997).
[14]K. Okamoto, H. Ohta, S. F. Chichibu, J. Ichihara, and H. Takasu, Jpn. J. Appl. Phys. **46**, L187 (2007).
[15]K. Kojima, M. Funato, Y. Kawakami, S. Masui, S. Nagahama, and T. Mukai, Appl. Phys. Lett. **91**, 251107 (2007).
[16]A. Tyagi, Y. D. Lin, D. A. Cohen, M. Saito, K. Fujito, J. S. Speck, S. P. DenBaars, and S. Nakamura, Appl. Phys. Express **1**, 091103 (2008).
[17]T. Kyono, Y. Yoshizumi, Y. Enya, M. Adachi, S. Tokuyama, M. Ueno, K. Katayama, and T. Nakamura, Appl. Phys. Express **3**, 011003 (2010).
[18]S. You, T. Detchprohm, M. Zhu, W. Hou, E. A. Preble, D. Hanser, T. Paskova, and C. Wetzel, Appl. Phys. Express **3**, 102103 (2010).
[19]S. Brinkley, Y. D. Lin, A. Chakraborty, N. Pfaff, D. Cohen, J. S. Speck, S. P. Denbaars, and S. Nakamura, Appl. Phys. Lett. **98**, 011110 (2011).
[20]F. Wu, Y. D. Lin, A. Chakraborty, H. Ohta, S. P. DenBaars, S. Nakamura, and J. S. Speck, Appl. Phys. Lett. **96**, 231912 (2010).
[21]H. Masui, H. Yamada, K. Iso, H. Hirasawa, N. N. Fellows, J. S. Speck, S. Nakamura, and S. P. DenBaars, Phys. Status Solidi A **205**, 1203 (2008).
[22]L. Schade, U. T. Schwarz, T. Wernicke, M. Weyers, and M. Kneissl, Phys. Status Solidi B **248**, 638 (2011).
[23]W. G. Scheibenzuber and U. T. Schwarz, Phys. Status Solidi B **248**, 647 (2011).
[24]M. Ueda, M. Funato, K. Kojima, Y. Kawakami, Y. Narukawa, and T. Mukai, Phys. Rev. B **78**, 233303 (2008).
[25]H. Masui, H. Asamizu, T. Tyagi, N. F. DeMille, S. Nakamura, and S. P. DenBaars, Appl. Phys. Express **2**, 071002 (2009).
[26]R. B. Chung, Y. D. Lin, I. Koslow, N. Pfaff, H. Ohta, J. Ha, S. P. DenBaars, and S. Nakamura, Jpn. J. Appl. Phys. **49**, 070203 (2010).
[27]See overview for information about the software. http://www.nextnano.de/nextnano3/
[28]Y. C. Chang and J. N. Schulman, Appl. Phys. Lett. **43**, 536 (1983).
[29]R. C. Miller, A. C. Gossard, G. D. Sanders, Y. C. Chang, and J. N. Schulman, Phys. Rev. B **32**, 12 (1983).
[30]D. J. Wolford, T. F. Kuech, J. A. Bradley, M. A. Gell, D. Ninno, and M. Jaros, J. Vac. Sci. Technol. B **4**, 4 (1986).
[31]M. C. Y. Chan, E. H. Li, and K. S. Chan, Physica B **245**, 317 (1998).
[32]Y. Zhao, S. C. Huang, C. Y. Huang, S. Tanaka, C. C. Pan, K. Fujito, D. Feezell, J. S. Speck, S. P. DenBaars, and S. Nakamura (unpublished).